ACS Medicinal Chemistry Letters

Letter

pubs.acs.org/acsmedchemlett

Discovery of MK-3168: A PET Tracer for Imaging Brain Fatty Acid Amide Hydrolase

Ping Liu,*[,†] Terence G. Hamill,[¶] Marc Chioda,[†] Harry Chobanian,[†] Selena Fung,[†] Yan Guo,[†] Linda Chang,[†] Raman Bakshi,[†] Qingmei Hong,[†] James Dellureficio,[†] Linus S. Lin,[†] Catherine Abbadie,[‡] Jessica Alexander,[‡] Hong Jin,[‡] Suzanne Mandala,[‡] Lin-Lin Shiao,[‡] Wenping Li,[¶] Sandra Sanabria,[¶] David Williams,[¶] Zhizhen Zeng,[¶] Richard Hajdu,[§] Nina Jochnowitz,[§] Mark Rosenbach,[§] Bindhu Karanam,[∥] Maria Madeira,[∥] Gino Salituro,[∥] Joyce Powell,[∥] Ling Xu,[∥] Jenna L. Terebetski,[⊥] Joseph F. Leone,[#] Patricia Miller,[¶] Jacquelynn Cook,[¶] Marie Holahan,[¶] Aniket Joshi,[¶] Stacey O'Malley,[¶] Mona Purcell,[¶] Diane Posavec,[¶] Tsing-Bau Chen,[¶] Kerry Riffel,[¶] Mangay Williams,[¶] Richard Hargreaves,[¶] Kathleen A. Sullivan,[‡] Ravi P. Nargund,[†] and Robert J. DeVita[†]

[†]Departments of Medicinal Chemistry, [‡]Immunology, [§]Pharmacology, [∥]Preclinical DMPK, [⊥]Basic Pharmaceutical Sciences, and [#]Process Research, Merck Research Laboratories, Rahway, New Jersey 07065, United States

[¶]Department of Imaging Research, Merck Research Laboratories, West Point, Pennsylvania 19486, United States

Supporting Information

ABSTRACT: We report herein the discovery of a fatty acid amide hydrolase (FAAH) positron emission tomography (PET) tracer. Starting from a pyrazole lead, medicinal chemistry efforts directed toward reducing lipophilicity led to the synthesis of a series of imidazole analogues. Compound **6** was chosen for further profiling due to its appropriate physical chemical properties and excellent FAAH inhibition potency across species. [^{11}C]-**6** (MK-3168) exhibited good brain uptake and FAAH-specific signal in rhesus monkeys and is a suitable PET tracer for imaging FAAH in the brain.

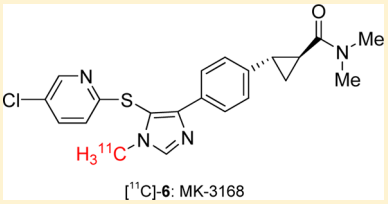

[^{11}C]-**6**: MK-3168

KEYWORDS: *Fatty acid amide hydrolase, FAAH, positron emission tomography, carbon-11, PET tracer, target engagement, biomarker*

Fatty acid amide hydrolase (FAAH) is a serine hydrolase characterized by an unusual Ser−Ser−Lys catalytic triad that cleaves amides and esters at similar rates.[1,2] It is an integral membrane enzyme responsible for the breakdown of several fatty acid ethanolamide (FAE) signaling molecules (Figure 1),

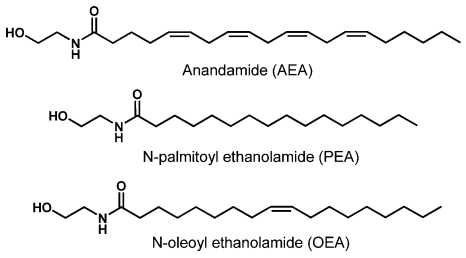

Figure 1. Substrates of fatty acid amide hydrolase.

including the endocannabinoid arachidonoyl ethanolamide (anandamide, AEA), and the related lipids *N*-palmitoyl ethanolamide (PEA) and *N*-oleoyl ethanolamide (OEA).[3−5] Inhibition of FAAH leads to elevated levels of these endogenous FAEs,[6] which act on cannabinoid, vanilloid, and other receptors to induce anti-inflammatory, antidepressant, analgesic, and anxiolytic effects in preclinical animal models.[7−9] In addition, these actions occur in the absence of the adverse effects typically observed with direct cannabinoid receptor agonists.[10,11] Thus, FAAH represents a potential therapeutic target for the treatment of pain, inflammation, and other clinical disorders. Indeed, a number of FAAH inhibitors have been reported including covalent, irreversible inhibitors; covalent, reversible inhibitors; and noncovalent, reversible inhibitors.[12−16] To better understand FAAH biology and assist in the design and testing of promising drug candidates targeting this enzyme, a suitable FAAH positron emission tomography (PET) or single photon emission computed tomography (SPECT) radioligand is highly desirable, which would allow FAAH imaging studies in the living human and animal brain under normal physiological and diseased conditions. In general, a successful PET ligand should provide a good specific signal (total/nonspecific ≥ 1.5:1) to allow quantitative mapping of the target of interest. Though not an absolute, ideally, a brain PET ligand should have a good binding affinity with $B_{max}/K_d \geq 10$ and reasonable lipophilicity with log *P* or log *D* of 1−3.5 for adequate brain penetration and optimum specific to nonspecific ratio.[17,18] Much effort has been devoted to the search for suitable FAAH PET ligands. The majority of the reported

Received: March 11, 2013
Accepted: April 20, 2013
Published: April 20, 2013

   dx.doi.org/10.1021/ml4000996 | ACS Med. Chem. Lett. 2013, 4, 509−513

radioligands are URB597 analogues[19,20] or anandamide analogues[21,22] (Figure 2). Recent reports have appeared for

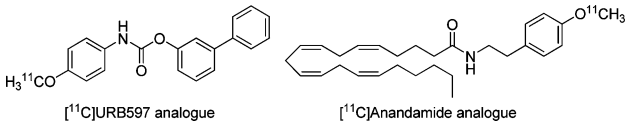

Figure 2. Representative examples of FAAH PET tracers.

[18F]PF-9811[23] and [11C-carbonyl]O-arylcarbamates[24] and the characterization of these tracers in rodents. Herein, we wish to report the discovery of a structurally distinct and reversible FAAH PET tracer (MK-3168) that may be suitable for clinical application.

The medicinal chemistry effort began with compound **2**,[25] a potent FAAH inhibitor that had been identified from our lead optimization program. Compound **2** has an HPLC log *D* value of 4.2 and subnanomolar FAAH inhibition potency across species. Although the lipophilicity of compound **2** is higher than desired, we were encouraged by its excellent potency and decided to radiolabel compound **2**. $^{11}CH_3$ was introduced through precursor **1** to yield [11C]-**2** (Scheme 1). However, in

Scheme 1. Initial Efforts for a FAAH PET Tracer

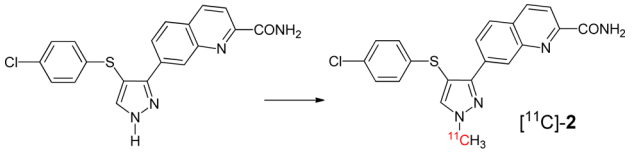

vivo PET studies of [11C]-**2** in rhesus monkeys were complicated by brain-penetrant and radiolabeled metabolites, suggesting the need for a different scaffold for radiolabeling.

Our attention shifted to compound **3**, another analogue from the pyrazole series[25] (Scheme 2). This compound has a reasonable FAAH inhibition potency in human and rat, but because rhesus monkey is our preferred preclinical species for evaluation of CNS PET tracers, its rhesus potency and lipophilicity required further optimization. More importantly, a reliable route to introduce a radiolabel to the molecule was needed since this was unable to be realized on compound **3**. Thus, our structure–activity relationship (SAR) objective was to modify structure **3** to decrease lipophilicity, improve potency, and locate a structural feature for efficient radiolabeling.

Replacing pyrazole with imidazole is an effective way to lower log *D*, provided other properties are maintained. In this regard, compound **4** (R = cyclopropyl) was synthesized; however, it was a much less potent compound (Scheme 2 and its table).[26] To our delight, when R was changed to methyl (compound **5**), the potency was improved by 3-fold; when R was removed (R = H; compound **6**), the potency was improved significantly. However, compound **7**, the imidazole regio isomer, and compound **8**, the uncapped imidazole analogue, reduced potency by about 100-fold. With the log *D* of compound **6** in an acceptable range, the methyl substituent on the imidazole could serve as a handle to introduce ^{11}C. To further lower the log *D*, primary amide **9** and secondary amide **10** were synthesized. While compound **9** was less potent than

Scheme 2. SAR Efforts and Identification of Compound 6

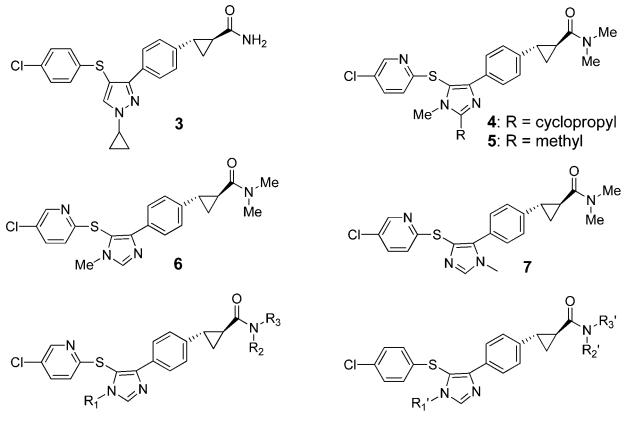

Cmpd	human[a] IC_{50} (nM)	rhesus[b,c] IC_{50} (nM)	rat[a] IC_{50} (nM)	HPLC Log D[b] (pH 7.3)
3	5.0 ± 0.9	33	4.2 ± 0.3	3.8
4	48 ± 4.3	nd	106 ± 1.8	nd
5	13.6 ± 1.1	nd	34 ± 2.2	nd
6	1.0 ± 0.6	5.5 ± 3.8[a]	1.7 ± 0.5	3.3
7	839 ± 145	nd	1388 ± 161	nd
8	650 ± 86	nd	145 ± 13	nd
9	3.3 ± 0.5	nd	12 ± 1.0	2.0
10	1.1 ± 0.3	nd	6.0 ± 1.6	2.9
11	3.2 ± 0.8	nd	4.8 ± 0.3	nd
12	1.5 ± 0.6	7.0	4.2 ± 0.3	3.0
13	3.0 ± 1.1	27	3.0 ± 0.7	3.4
14	0.3 ± 0.1	1.4	0.6 ± 0.2	4.2
15	0.8 ± 0.2	nd	1.7 ± 0.1	3.6
16	0.5 ± 0.1	nd	1.4 ± 0.0	3.8
17	1.0 ± 0.3	3.1	1.4 ± 0.1	4.0
18	1.1 ± 0.4	8.8	1.3 ± 0.4	4.3

[a]FAAH inhibition IC_{50} data expressed as mean ± SD ($n \geq 2$ independent experiments). [b]nd = not determined. [c]Assayed only once except for compound **6**.

compound **6**, compound **10** offered comparable potency. Furthermore, to consider the option of introducing ^{18}F to the molecule, fluoroethyl analogues **11**–**13** were synthesized. Compounds **11** and **12** could be candidates for a ^{18}F PET tracer, but analogue **13** was not an option due to its poor potency in rhesus, which is our preferred preclinical species for imaging studies. Finally, to complete the SAR studies, the chlorophenyl analogues **14**–**18** were also synthesized. These chlorophenyl analogues offered better potency (for example, **14** vs **6**) but increased lipophilicity.

Compound **6** was chosen for further profiling. In the whole blood FAAH inhibition assay, compound **6** exhibited excellent potency in human (IC_{90} = 5.5 nM) and rhesus (IC_{90} = 29 nM). An off-target screen of this compound was performed against a panel of 168 receptors, ion channels, and enzymes; only two off-target activities, acetyl cholinesterase (IC_{50} = 1.63 μM) and phosphodiesterase PDE4 (IC_{50} = 9.75 μM), were identified. Compound **6** was very selective over the two key ion channels, hERG (IC_{50} = 37 μM) and DLZ (IC_{50} = 16 μM); CYP 3A4 (IC_{50} > 50 μM); as well as the two cannabinoid receptors, CB1 (IC_{50} = 30 μM) and CB2 (IC_{50} = 150 μM). This compound was not a substrate for rat or human P-glycoprotein in vitro and rapidly penetrated into the brain and achieved a brain-to-

dx.doi.org/10.1021/ml4000996 | ACS Med. Chem. Lett. 2013, 4, 509–513

plasma concentration ratio of 7:1 at 2 h following a 2 mg/kg oral dose to rats. On the basis of its overall profile, we believed compound **6** would provide a high probability of success to develop as a ^{11}C PET tracer.

The synthesis of [^{3}H]-**6** and [^{11}C]-**6** is outlined in Scheme 3 and began with a Negishi-type coupling[27] between chiral

Scheme 3. Synthesis of [^{3}H]-6 and [^{11}C]-6[a]

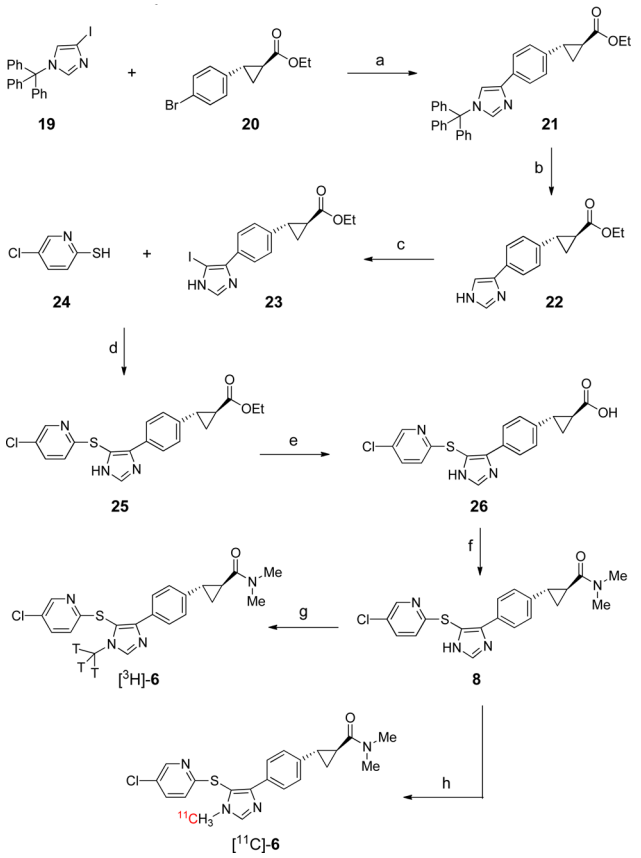

[a]Reagents and conditions: (a) **19**, EtMgBr, $ZnCl_2$ in THF, then **20** and $Pd(PPh_3)_4$, reflux, 72%; (b) 1 N HCl, MeOH, reflux, 66%; (c) NIS, dichloromethane, rt, 53%; (d) CuI, 1,10-phenanthroline, DMSO, 100 °C, 26%; (e) KOH, MeCN/water, 80 °C; (f) dimethylamine, HOBT, EDC, diisopropylethylamine, DMF, 72% for 2 steps; (g) CT_3I, Cs_2CO_3, DMF, rt; (h) [^{11}C]-MeI, Cs_2CO_3, DMF, 65 °C.

bromide **20**[28] and the zinc species derived from the commercially available **19**. This C−C bond formation provided compound **21** in 72% yield. After the trityl group was removed with HCl, imidazole **22** was converted by NIS to iodoimidazole **23** that was ready for the C−S bond formation. This C−S coupling proved challenging, most likely due to the interference of the free imidazole N−H.[29] In the end, the CuI-mediated coupling conditions were used for the reaction between iodoimidazole **23** and thiol **24**[28] that afforded sulfide **25** in 26% yield. With intermediate **25** in hand, the remaining synthesis was straightforward. Ester hydrolysis and amide formation gave **8**, a precursor to both [^{3}H]-**6** and [^{11}C]-**6**. Reaction of **8** with CT_3I provided [^{3}H]-**6**. Finally, **8** was reacted with [^{11}C]-CH_3I completing the synthesis of PET tracer [^{11}C]-**6**.[30]

[^{3}H]-**6** was used in tissue homogenate binding studies. As shown in Table 1, compound **6** exhibited excellent binding affinity to the cortex of rat, rhesus, and human. In addition,

Table 1. Tissue homogenate binding studies[a] with [^{3}H]-6

tissue	K_d (nM)	B_{max} (nM)	B_{max}/K_d
rat cortex	0.6 ± 0.1	43 ± 4	73 ± 11
rhesus cortex	1.4 ± 0.2	21 ± 3	15 ± 1
human cortex	0.8 ± 0.2	15 ± 1	19 ± 6

[a]Data expressed as mean ± SD (n = 3 independent experiments).

Scatchard plot of transformed data showed that [^{3}H]-**6** bound to a single, saturable site in these species.[31] More importantly, the comparable B_{max}/K_d ratio for rhesus monkey and human suggested that the magnitude of an observed in vivo specific signal of [^{11}C]-**6** in rhesus monkey could be similar to that in human.

The pharmaceutical properties of compound **6** were also assessed and the crystalline free base was characterized as its solid state form. This form of compound **6** showed excellent 24 h pH dependent solution stability, and solubility values obtained in 10 mM saline buffer at pH 3−8, with 10% ethanol, should provide adequate solubility to support clinical iv dosing.

[^{11}C]-**6** was evaluated in isoflurane-anesthetized rhesus monkeys as a potential PET ligand. Baseline scans after a single iv (5 mCi) administration revealed that [^{11}C]-**6** rapidly penetrated the blood/brain barrier and accumulated in the frontal cortex, striatum, and hippocampus regions (FAAH enriched area),[32] reaching a maximum signal in ∼45 min. A blockade experiment was also carried out with compound **2**, a potent FAAH inhibitor in rhesus (Figure 3). The total to

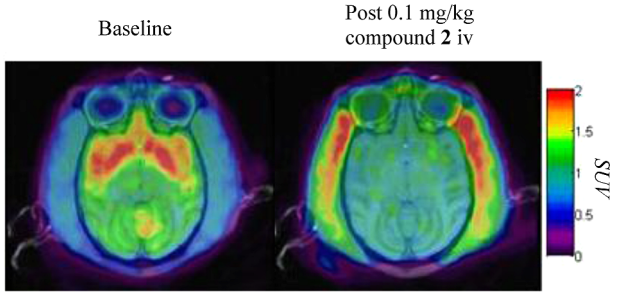

Summed images 60-90 min post tracer injection normalized to white-matter uptake, SUV.

Figure 3. In vivo PET images of [^{11}C]-**6** in rhesus monkey brain. Color scale indicates standard uptake value (SUV) units (nCi/cc/mCi/kg).

nonspecific signal ratio was ∼2:1, exceeding the targeted criteria 1.5:1. Table 2 compares the profile of [^{11}C]-**6** against our target

Table 2. Comparison of Target Criteria and Profile of [^{11}C]-6

target criteria for a FAAH PET tracer	[^{11}C]-**6** profile
human B_{max}/K_d > 10	19
human K_d < 2 nM	0.8
moderate log D (1−3.5)	3.3
non- or weak substrate for hPGP (MDR)	0.8
Papp > 20 × 10^{-6} cm/s[a]	27 × 10^{-6} cm/s
reliable route for C-11 or F-18 labeling	[^{11}C]-MeI
good brain uptake in monkey	>1 SUV[b]
specific signal ≥ 1.5:1 (total/nonspecific)	∼2:1

[a]Measurement of cell permeability. [b]SUV: nCi/cc/mCi/kg body weight.

dx.doi.org/10.1021/ml4000996 | ACS Med. Chem. Lett. 2013, 4, 509−513

criteria for a FAAH PET tracer. We believe [^{11}C]-**6** has the criteria of a successful FAAH PET tracer and should find wide use for in vivo FAAH PET studies.

In summary, a high quality FAAH PET tracer [^{11}C]-**6** (MK-3168) was developed through optimization of lipophilicity and potency for FAAH inhibition of the initial lead compound. This PET tracer exhibited good brain uptake and FAAH-specific signal in rhesus monkey PET studies and therefore was a suitable PET tracer for imaging FAAH in the brain. These results led to the decision to investigate [^{11}C]-**6** in the clinic, which will be the subject of another publication.

■ ASSOCIATED CONTENT

Supporting Information

Synthetic procedures and characterization data of selected compounds, conditions for the biological assays, reversibility study of compound **6**, and protocol for rhesus PET imaging. This material is available free of charge via the Internet at http://pubs.acs.org.

■ AUTHOR INFORMATION

Corresponding Author

*(P.L.) Phone: 732-594-0321. Fax: 732-594-9556. E-mail: ping_liu2@merck.com.

Notes

The authors declare no competing financial interest.

■ ACKNOWLEDGMENTS

We thank the department of Laboratory Animal Resources for their assistance in animal dosing and sampling.

■ REFERENCES

(1) Ahn, K.; McKinney, M. K.; Cravatt, B. F. Enzymatic pathways that regulate endocannabinoid signaling in the nervous system. *Chem. Rev.* **2008**, *108*, 1687−1707.

(2) McKinney, M. K.; Cravatt, B. F. Structure and function of fatty acid amide hydrolase. *Annu. Rev. Biochem.* **2005**, *74*, 411−432.

(3) Lambert, D. M.; Vandevoorde, S.; Jonsson, K. O.; Fowler, C. J. The palmitoylethanolamide family: A new class of anti-inflammatory agents? *Curr. Med. Chem.* **2002**, *9*, 663−674.

(4) Devane, W. A.; Hanus, L.; Breuer, A.; Pertwee, R. G.; Stevenson, L. A.; Griffin, G.; Gibson, D.; Mandelbaum, A.; Etinger, A.; Mechoulam, R. Isolation and structure of a brain constituent that binds to the cannabinoid receptor. *Science* **1992**, *258*, 1946−1949.

(5) Rodriguez de Fonseca, F.; Navarro, M.; Gomez, R.; Escuredo, L.; Nava, F.; Fu, J.; Murillo-Rodriguez, E.; Giuffrida, A.; LoVerme, J.; Gaetani, S.; Kathuria, S.; Gall, C.; Piomelli, D. An anorexic lipid mediator regulated by feeding. *Nature* **2001**, *414*, 209−212.

(6) Cravatt, B. F.; Demarest, K.; Patricelli, M. P.; Bracey, M. H.; Giang, D. K.; Martin, B. R.; Lichtman, A. H. Supersensitivity to anandamide and enhanced endogenous cannabinoid signaling in mice lacking fatty acid amide hydrolase. *Proc. Natl. Acad. Sci. U.S.A.* **2001**, *98*, 9371−9376.

(7) Lichtman, A. H.; Shelton, C. C.; Advani, T.; Cravatt, B. F. Mice lacking fatty acid amide hydrolase exhibit a cannabinoid receptorme-diated phenotypic hypoalgesia. *Pain* **2004**, *109*, 319−327.

(8) Gaetani, S.; Dipasquale, P.; Romano, A.; Righetti, L.; Cassano, T.; Piomelli, D.; Cuomo, V. The endocannabinoid system as a target for novel anxiolytic and antidepressant drugs. *Int. Rev. Neurobiol.* **2009**, *85*, 57−72.

(9) Gobbi, G.; Bambico, F. R.; Mangieri, R.; Bortolato, M.; Campolongo, P.; Solinas, M.; Cassano, T.; Morgese, M. G.; Debonnel, G.; Duranti, A.; Tontini, A.; Tarzia, G.; Mor, M.; Trezza, V.; Goldberg, S. R.; Cuomo, V.; Piomelli, D. Antidepressant-like activity and modulation of brain monoaminergic transmission by blockade of anandamide hydrolysis. *Proc. Natl. Acad. Sci. U.S.A.* **2005**, *102*, 18620−18625.

(10) Kathuria, S.; Gaetani, S.; Fegley, D.; Valino, F.; Duranti, A.; Tontini, A.; Mor, M.; Tarzia, G.; La Rana, G.; Calignano, A.; Giustino, A.; Tattoli, M.; Palmery, M.; Cuomo, V.; Piomelli, D. Modulation of anxiety through blockade of anandamide hydrolysis. *Nat. Med.* **2003**, *9*, 76−81.

(11) Piomelli, D. The molecular logic of endocannabinoid signalling. *Nat. Rev. Neurosci.* **2003**, *4*, 873−884.

(12) Ahn, K.; Johnson, D. S.; Cravatt, B. F. Fatty acid amide hydrolase as a potential therapeutic target for the treatment of pain and CNS disorders. . *Expert Opin. Drug Discovery* **2009**, *4*, 763−784.

(13) Minkkila, A.; Saario, S.; Nevalainen, T. Discovery and development of endocannabinoid-hydrolyzing enzyme inhibitors. *Curr. Top. Med. Chem.* **2010**, *10*, 828−858.

(14) Seierstad, M.; Breitenbucher, J. G. Discovery and development of fatty acid amide hydrolase (FAAH) inhibitors. *J. Med. Chem.* **2008**, *51*, 7327−7343.

(15) Otrubova, K.; Ezzili, C.; Boger, D. L. The discovery and development of inhibitors of fatty acid amide hydrolase (FAAH). *Bioorg. Med. Chem. Lett.* **2011**, *21*, 4674−4685.

(16) Scott, C. W.; Tian, G.; Yu, X. H.; Paschetto, K. A.; Wilkins, D. E.; Meury, L.; Cao, C. Q.; Varnes, J.; Edwards, F. D. Biochemical characterization and in vitro activity of AZ513, a noncovalent, reversible, and noncompetitive inhibitor of fatty acid amide hydrolase. *Eur. J. Pharmacol.* **2011**, *667*, 74−79.

(17) Eckelman, W. C.; Gibson, R. E.; Rzeszotarski, W. J.; Vieras, F.; Mazaitis, J. K.; Francis, B.; Reba, W. C. The Design of Receptor Binding Radiotracers. In *Principles of Radiopharmacology*; Colombetti, L., Ed.; CRC Press: New York, 1979; Vol. *1*, pp 251−274.

(18) Waterhouse, R. N. Determination of lipophilicity and its use as a predictor of blood-brain barrier penetration of molecular imaging agents. *Mol. Imaging Biol.* **2003**, *5*, 376−389.

(19) Wyffels, L.; Muccioli, G. G.; Kapanda, C. N.; Labar, G.; De Bruyne, S.; De Vos, F.; Lambert, D. M. PET imaging of fatty acid amide hydrolase in the brain: synthesis and biological evaluation of an ^{11}C-labelled URB597 analogue. *Nucl. Med. Biol.* **2010**, *37*, 665−675.

(20) Wilson, A. A.; Garcia, A.; Parkes, J.; Houle, S.; Tong, J.; Vasdev, N. [^{11}C]CURB: Evaluation of a novel radiotracer for imaging fatty acid amide hydrolase by positron emission tomography. *Nucl. Med. Biol.* **2011**, *38*, 247−253.

(21) Wyffels, L.; Muccioli, G. G.; De Bruyne, S.; Moerman, L.; Sambre, J.; Lambert, D. M.; De Vos, F. Synthesis, in vitro and in vivo evaluation, and radiolabeling of aryl anandamide analogues as candidate radioligands for in vivo imaging of fatty acid amide hydrolase in the brain. *J. Med. Chem.* **2009**, *52*, 4613−4622.

(22) Wyffels, L.; De Bruyne, S.; Blanckaert, P.; Lambert, D. M.; De Vos, F. Radiosynthesis, in vitro and in vivo evaluation of ^{123}I-labeled anandamide analogues for mapping brain FAAH. *Bioorg. Med. Chem.* **2009**, *17*, 49−56.

(23) Skaddan, M. B.; Zhang, L.; Johnson, D. S.; Zhu, A.; Zasadny, K. R.; Coelho, R. V.; Kuszpit, K.; Currier, G.; Fan, K.-H.; Beck, E. M.; Chen, L.; Drozda, S. E.; Balan, G.; Niphakis, M.; Cravatt, B. F.; Ahn, K.; Bocan, T.; Villalobos, A. The synthesis and in vivo evaluation of [^{18}F]PF-9811: a novel PET ligand for imagingbrain fatty acid amide hydrolase (FAAH). *Nucl. Med. Biol.* **2012**, *39*, 1058−1067.

(24) Wilson, A. A.; Hicks, J. W.; Sadovski, O.; Parkes, J.; Tong, J.; Houle, S.; Fowler, C. J.; Vasdev, N. Radiosynthesis and evaluation of [^{11}C-carbonyl]-labeled carbamatesas fatty acid amide hydrolase radiotracers for positron emission tomography. *J. Med. Chem.* **2013**, *56*, 201−209.

(25) The medicinal chemistry efforts on the pyrazole series is the subject of another publication.

(26) The potency drop was primarily due to the core change. There were two other changes from **3** to **4**: chlorophenyl changed to chloropyridyl; primary amide changed to *N*,*N*-dimethyl tertiary amide. The former slightly decreased potency, and the latter slightly increased potency. They should cancel each other. Chloropyridyl was used here to further lower Log D.

(27) Negishi, E.-I.; Hu, Q.; Huang, Z.; Wang, G.; Yin, N. Palladium- or Nickel-Catalyzed Cross-Coupling Reactions with Organozincs and Related Organometals. In *Chemistry of Organozinc Compounds*; Wiley: New York, 2006; Part 1, pp 457−553.
(28) For its synthesis, see Supporting Information.
(29) During the synthesis of the cold **6**, the similar C−S coupling between methyl capped **23** and thiol **24** was high yielding (see Supporting Information).
(30) The methylation of imidazole **8** to product **6** was highly regioselective where the regioisomer **7** was unable to detect from the crude product by NMR. In fact, compound **7** had to be prepared by a different route (see Supporting Information).
(31) Dahlquist, F. W. The meaning of Scatchard and Hill plots. *Methods Enzymol.* **1978**, *48*, 270−299.
(32) Ueda, N.; Puffenbarger, R. A.; Yamamoto, S.; Deutsch, D. G. The fatty acid amide hydrolyse (FAAH). *Chem. Phys. Lipids* **2000**, *108*, 107−121.